Composites Part B 164 (2019) 675–682

Contents lists available at ScienceDirect

Composites Part B

journal homepage: www.elsevier.com/locate/compositesb

# Superior electro-optics of nano-phase encapsulated liquid crystals utilizing functionalized carbon nanotubes

Srinivas Pagidi[a], Ramesh Manda[a], Surjya Sarathi Bhattacharyya[b], Kyeong Jun Cho[a], Tae Hyung Kim[a], Young Jin Lim[a], Seung Hee Lee[a,*]

[a] Applied Materials Institute for BIN Convergence, Department of BIN Convergence Technology and Department of Polymer Nano Science and Technology, Chonbuk National University, Jeonju, Jeonbuk, 54896, Republic of Korea
[b] Asutosh College, 92, Shyamaprasad Mukherjee Road, Kolkata, 700 026, West Bengal, India

ARTICLE INFO

*Keywords:*
Optically isotropic liquid crystal
Polymer-matrix composites
Functionalized carbon nanotube

ABSTRACT

Nano-size distribution of birefringent liquid crystal droplets embedded in the polymer matrix gives rise to an optically isotropic liquid crystal (OILC) phase and the device utilizing OILC composite opens the possibility of alignment layer-free, flexible liquid crystal displays with fast response time. However, few critical issues such as high operating voltages and feeble light scattering are remained to be overcome before their widespread applications. To rectify the drawbacks, a small amount of conductive and anisotropic functionalized carbon nanotubes (f-CNTs) is doped into conventional OILCs. Consequently, switchable electro-optic properties of the proposed approach reveal that driving voltage is decreased by18.7%, response time becomes fast by 27%, and feeble light leakage is reduced to around 3.8 times, compared to conventional one, which helps the proposed approach to be competitive for display and photonic applications of film type of OILCs.

## 1. Introduction

For the past few decades, the flat panel type - liquid crystal displays (LCDs) were successfully commercialized for various applications. In recent years plastic organic light emitting diodes (POLEDs) are quite fascinated owing to their free designing structures with flexibility, bendability, and foldability. For attracting the people's attention towards LCDs and to compete with the POLEDs, binary composite systems of the optically isotropic liquid crystals (OILCs) have been introduced, in which the nanostructured LC droplets are obtained, upon UV polymerization. The superior performances of OILCs include the fast response time, wide-temperature range in the optically isotropic state, alignment layer-free, and wide-viewing angle [1–6]. In addition, the displayed image qualities in the conventional LCDs change very easily when the display is either under external pressure or bent, however, the LCDs with OILCs can overcome such difficulties because a fluid nematic LC is encapsulated in a nanostructured polymer matrix so that their electro-optic properties are preserved even in either curved or bent state. However, despite these merits, high driving voltages and feeble light scattering in a voltage-off black state are still hindering towards potential applications.

The OILCs can be obtained by the well-known method of polymerization induced phase stabilization (PIPS), at ambient conditions [4,7,8]. With optimization of LC to monomer ratio, UV exposure conditions and materials, the size of phase-separated LC droplets can be realized to be below the visible wavelength regime [6,9–11], and the LC directors inside droplets are randomly oriented from droplet to droplet, giving rise to an optically isotropic phase at field-off state. Consequently, when the OILCs tested under crossed polarizers, it appears to be a dark state and then birefringence is induced in the field-on state, giving rise to a bright state. In OILCs, more than 50 wt.% of the photocurable monomer is used to minimize the light scattering and due to this reason, [12,13] thicker polymer matrix between the isotropic droplets with a low filling factor of LC droplets has been realized. Besides, the dielectric constant of the polymer matrix drops down the Kerr constant ($K$) of the OILC system $\sim 7.53 \times 10^{-10}$ m/V$^2$ rendering driving voltage of the device high [4].

In recent years, several approaches were proposed to lower operating voltage of OILCs. Among them, one was to obtain higher K ($\sim$1 nm/V$^2$) using a LC with high dielectric anisotropy and birefringence [14] and the other was using the flexible/week anchoring pre-polymers with relative diluents [15,16]. Most recently, we have reported solutions to solve the feeble light scattering by dispersing a small amount of chiral dopant to nano-PDLCs [17] and using acrylate

* Corresponding author.
*E-mail address:* lsh1@chonbuk.ac.kr (S.H. Lee).

https://doi.org/10.1016/j.compositesb.2019.01.091
Received 23 December 2018; Received in revised form 14 January 2019; Accepted 18 January 2019
Available online 25 January 2019
1359-8368/ 

monomer PN393 [18]. Despite of great efforts, the high driving voltage is still an unsolved problem for the practical application. To address the above challenges, it is viable either to utilize more LC concentration in the composite or to enhance the conductivity of the composite. Increasing LC content is not advisable, because larger droplets lead a feeble incident light scattering. Therefore, we challenge to lower the driving voltage by increasing the conductivity of a polymer matrix.

In recent times, the anisotropic electrical conductivity and magnetic properties of CNTs are gaining more and more curiosity among the researchers worldwide [19,20]. In addition, high aspect ratio acts as a better dopant for improving their properties of the composite matrix [21,22]. Owing to such merits, highly conductive CNTs are considered as a promising candidate for incorporating into the composite. However, the naïve CNTs are much prone to form agglomerations due to stronger van der Waals interactions between them. Therefore, it is quite a difficult task for developing a composite film with uniform dispersion. In the present investigation, acid functionalized CNTs (f-CNTs) are used as a dopant to form a uniform composite and the effects of f-CNTs on the surface morphological and switchable electro-optical properties of OILC-LCDs are studied in detail. The result implies that the effect of doped f-CNTs enables to reduce efficiently the threshold ($V_{th}$) and driving ($V_{op}$) voltages with faster switching times. In addition, an efficient dark state in the device was realized.

## 2. Experimental

### 2.1. Materials and preparation method of f-CNT doped OILC composites

The OILC mixture is composed of high dielectric anisotropy nematic LC and the conventional thiolene type of monomer. We have used MLC-2053 (dielectric anisotropy $\Delta\varepsilon = 42.6$, $T_{NI} = 86\,^{\circ}C$, birefringence $\Delta n = 0.235$ at 589.3 nm, from Merck Advanced Technology, Korea) as nematic LC, and conventional NOA-65 (Norland Optical Adhesive 65, $n_p = 1.514$ at 20 °C and 589 nm) as pre-polymer for OILC preparation. The OILC and its composites consist of 45% of LC and 55% of NOA-65 and added various concentrations of the f-CNTs of $1 \times 10^{-3}$, $5 \times 10^{-3}$ and $1 \times 10^{-2}$ wt. %. Hereafter, the OILC sample is named as S1 and composite samples are named as S2, S3, and S4, respectively, following the order of increased concentration of doped f-CNT. The composites were heated to an isotropic temperature of the mixture i.e. 90 °C and ultra-sonication was performed for 180 min. As the elevated temperature helps to reduce the viscosity of pre-polymer, an enhanced degree of dispersion is anticipated. The mixtures were filled into the IPS cells at isotropic temperature. Subsequently, the cells were exposed to UV intensity of 140 mW/cm$^2$ for 6mins, for photopolymerization. A schematic diagram for the preparation of the f-CNTs doped OILC composite is illustrated in Fig. 1. The polymerization kinetics plays a prominent role because the phase separation mainly depends on the curing intensity, curing time and thermal stability of the system [22]. To avoid such intrinsic difficulties all samples were irradiated one after other without changing the UV light intensity and the temperature conditions. Electro-optic properties of the samples have been investigated by filling the samples in interdigitated patterned electrodes of single domain IPS cells. The width ($w$) of the ITO electrode is 4 μm and distance ($l$) is 4 μm between electrodes. The cell was assembled together with a silicon ball spacer of 10 μm.

### 2.2. Acid functionalization of SWCNTs

Single-walled carbon nanotubes (CNTs) having diameter ~ 1.1 nm and length ~ 1–3 μm (Avention. Co. Ltd. Korea) were utilized for our experiments. However, the pristine CNTs form clusters when adopted into a high viscous pre-polymer because they are prone to form agglomerates due to stronger van der Waals forces. Therefore, the surface chemical modification was done by acidification process which also reduces their size. To make surface functionalization, 5 mg of pristine CNT was suspended into 2.5 ml concentrated acid mixture of $H_2SO_4$ and $HNO_3$ (volume ratio 3:1) and then ultra-sonication was performed for 3 h. Thereafter, the CNTs suspended mixture was washed several times using distilled water to neutralize solute followed by centrifuging in 12,000 rpm for 25mins. The resultant mixture was placed in oven drying for 1 h at 150 °C giving rise to the CNT powder. Finally, the powder is dispersed into acetone by ultrasonication for 30mins, hereafter, they named as f-CNTs. The obtained f-CNTs are characterized using the TEM, as shown in the photomicrograph of Fig. 2.

### 2.3. Characterization techniques

To investigate the optical and field-responsive properties of pure and doped OILCs several characterization techniques were performed. The polarizing optical microscope (POM) (Nikon, ECLIPSE E600, Japan) attached with CCD camera (Nikon, DXM 1200), was used to observe its isotropic phase and induced birefringence upon field-on state between crossed polarizers. The POM images obtained at field-off state were utilized for the quantitative analysis of light leakage in the dark state by using *i*-solution software (*i*-solution Inc., *i*M Technology, Korea). The electro-optic properties were measured as a function of the applied voltage by using a lab-made set-up under crossed polarizers. The field was applied to the IPS cell using a function generator (Agilent 33521A) and the change in transmitted light intensity was detected by photo-detector and the data were collected using an oscilloscope (Tektronix DPO 2024B). The wavelength-dependent transmission was measured using the UV-Visible spectroscopy (SCINCO, S-3100) from ultraviolet to near infrared region. Finally, the surface morphology of the LC removed polymer network was characterized using the field emission scanning electron microscope (FE-SEM).

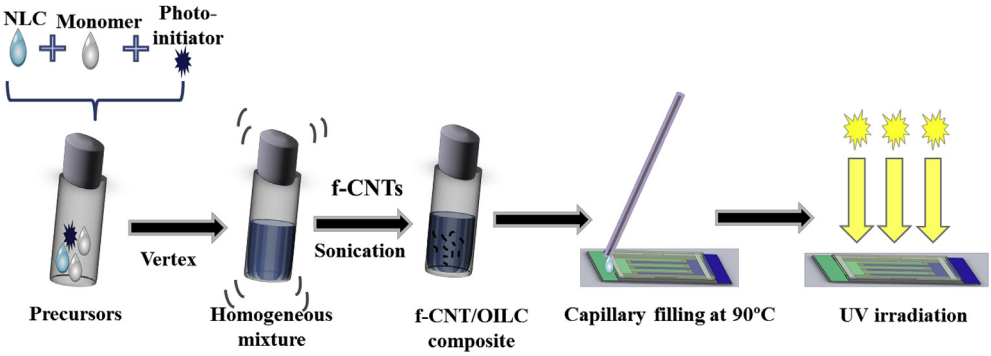


**Fig. 1.** Schematic illustration for the formation of f-CNTs doped OILC composites.

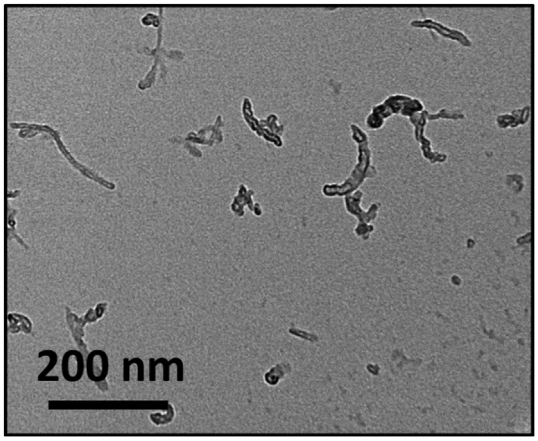


**Fig. 2.** A TEM image of the acid functionalized SWCNTs (f-CNTs).

## 3. Fabrication of f-CNT doped OILC-LCD and its switching mechanism

Realization of visible light scattering free OILC film is necessary to minimize light loss and enhance the contrast ratio of liquid crystal display and photonic device. However, the use of relatively high pre-polymer concentration is inevitable to get OILC film with the size of LC droplets less than 250 nm in PIPS approach. This leads to thick polymeric walls encapsulating and isolating LC droplets, resulting in a low filling factor of LC molecules in the composite. Consequently, on field application, the field inside the polymeric dielectric media experiences screening effect by the high dielectric constant of the polymer matrix. In addition, the field screening is proportional to the thickness and inversely proportional to the dielectric constant of the polymer matrix, so that utilization of high concentration of the polymer results in reducing $K$ of the composite. Therefore, higher $V_{th}$ and $V_{op}$ are required to induce the maximum phase retardation in the OILCs [23,24].

In order to overcome such shortcomings in the OILC with PIPS approach, we have incorporated conductive f-CNTs into the conventional OILCs to realize better electro-optic performed LCDs. We anticipate most of the f-CNTs are wrapped in a polymer matrix and few of them are immersed in LC droplets as depicted in the schematic diagram Fig. 3. The incorporation of f-CNTs into droplets is naturally inhibited by their sizes. However, one can anticipate considerable dispersion in length of CNTs after functionalizing chemical treatments. Hence a few of f-CNTs whose length is smaller than droplet size might be fully submerged inside the LC droplet. In that case, f-CNTs mostly follow the long-range ordering of the LC director and reorient along the field direction when the field is applied, while the dispersed ones in a polymer matrix do not respond to the applied field. Short-range elastic interactions between LCs and f-CNTs inside the droplet may result in shorter decay response time owing to an increased elastic constant. Additionally, polymer wrapped f-CNTs provide high degrees of interconnections between the isolated LC droplets. Consequently, the field strength inside the dielectric media is significantly enhanced resulting in the reduced $V_{th}$ and $V_{op}$.

The $V_{th}$ of the f-CNTs doped OILCs varies with the concentration of the dopant in the composite. Therefore, the modified $V_{th}$ can be expressed as [25],

$$V_{th} = \frac{1}{c}\frac{\pi l}{R}\sqrt{\frac{k_{eff}}{\varepsilon_o \Delta\varepsilon}}, \tag{1}$$

where $l$ is the distance between the adjacent electrodes in the IPS cell, $k_{eff}$ is the elastic constant (mainly associated with both $k_{11}$ and $k_{33}$), $\varepsilon_o$ is the dielectric permittivity of free space, $\Delta\varepsilon$ is the dielectric anisotropy of the host LC, $R$ is the droplet size of LC and '$c$' is the prefactor defined as,

$$c = \frac{3\varepsilon_M}{\varepsilon_{LC} + 2\varepsilon_M},$$

where $\varepsilon_M$ is the effective dielectric constant of the polymer matrix and $\varepsilon_{LC}$ is the dielectric constant of the host LC. Considering mono-dispersed droplet size for the fixed LC concentration, the magnitude of $c$ enhances with the doping concentration of f-CNTs and reduces $V_{th}$ by equation (1). Thus the increased conductivity of the matrix by f-CNT doping could play a predominant role in reducing the driving voltages, at given physical properties of LCs and device. Furthermore, the decay time ($\tau_{off}$) of the device is given by Ref. [26],

$$\tau_{off} \approx \frac{\gamma_1 R^2}{k_{eff}\pi^2}, \tag{2}$$

where $\gamma_1$ is the rotational viscosity of the host LC, and $k_{eff}$ is the effective elastic deformation. If $k_{eff}$ of LC is increased by doped CNT, $\tau_{off}$ can be shorter [27],

In addition to the effects of f-CNT doping on electro-optics, a considerable fraction of absorption by CNTs can be realized when the incident light propagates through the composite medium. In such situations, the transmittance light intensity ($I_T$) through the OILC film can be described by Beer-Lambert law, which can be expressed as [28],

$$\frac{I_T}{I_I} = e^{-(\alpha+\beta)d}, \tag{3}$$

where $I_I$ is the incident light intensity, $\alpha$ and $\beta$ are the scattering and

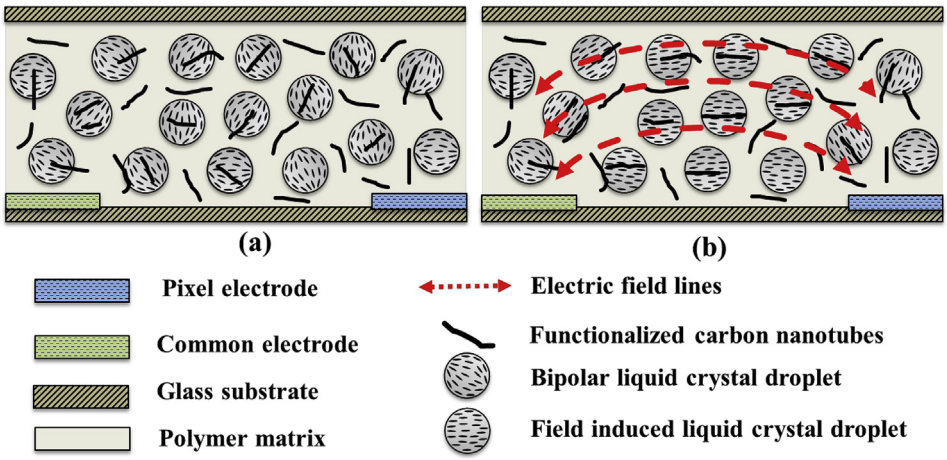


**Fig. 3.** Schematic diagram of the doped f-CNTs into OILC: (a) Random distribution LC directors with f-CNTs in the polymer matrix in voltage-off state and (b) LC directors and f-CNTs inside the droplets align to the field direction whereas f-CNTs in the polymer matrix do not reorient in voltage-on state.

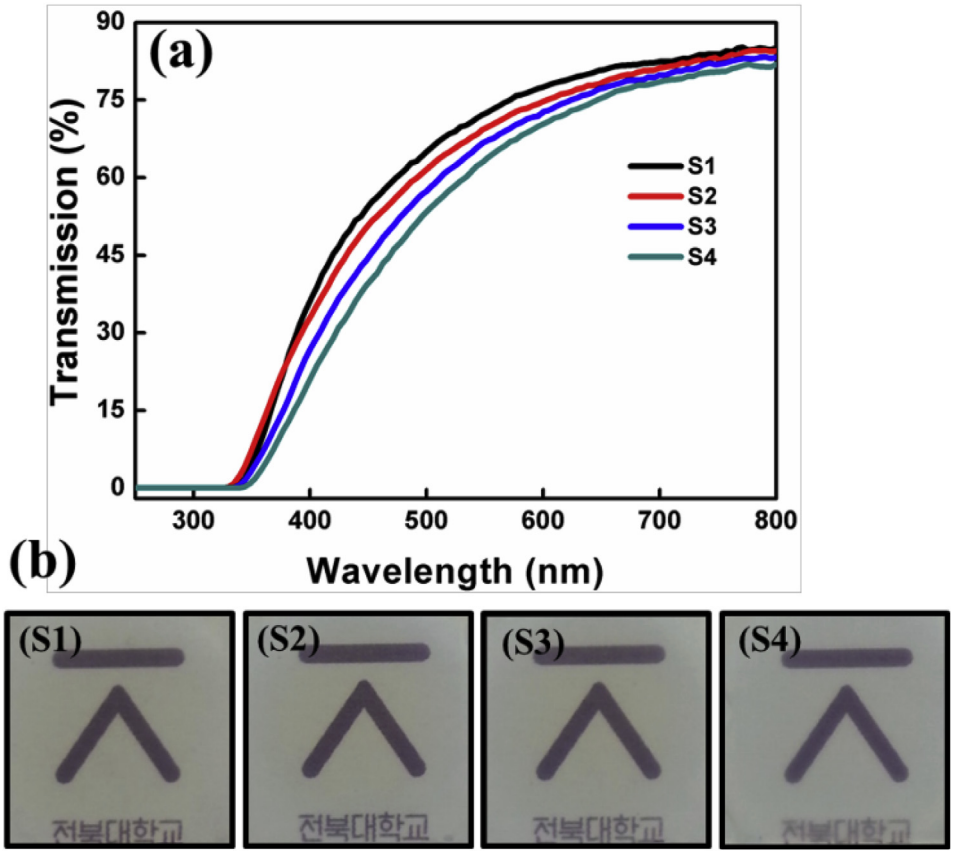


**Fig. 4.** (a) Wavelength-dependent transmission spectra and (b) High-resolution macro-images of the f-CNTs doped OILCs indicating the transmittance decreases with increasing doping of f-CNT.

absorbance coefficients of the composite film, respectively and $d$ is the film thickness. The scattering coefficient ($\alpha$) mainly relies on the $\rho_s$ density of LC droplets and scattering cross-sectional area ($\sigma_s$). According to the Rayleigh-Gans scattering theory, the average $\sigma_s$ is inversely proportional to the fourth power of wavelength of incident light ($\lambda^4$) [29]. The absorption coefficient ($\beta$) of the film can be expressed as, $\beta = \varepsilon x l'$, where $\varepsilon$ is coefficient of absorptivity of the doping material, $x$ is the concentration of dopant and $l'$ is the ratio of the distance traveled by light through the film thickness ($d$). The f-CNTs can absorb the incident [30] and any scattered light inside the OILC phase, playing role of absorbing dopant such that the feeble light leakage is significantly suppressed under the crossed polarizers.

## 4. Results and discussions

### 4.1. Ultraviolet-visible (UV-Visible) and surface morphological properties

UV-Visible transmittance profiles of all the samples in the wavelength range from 300 to 800 nm were investigated, as shown in Fig. 4(a). The spectrum depicts that the transmittance increases with increasing wavelength of the incident light because of $\sigma_s \propto 1/\lambda^4$ i.e., the shorter wavelength the light scatters more. In addition, the transmittance slightly decreases with increasing doping concentration of f-CNTs such that the measured transmission for the samples S1 to S4 is 78.58, 76.9, 75.29 and 74.6% at 630 nm. The high-resolution photographic images were captured under the ambient illumination without using the polarizers as depicted in Fig. 4(b). Evidently, the transmitted light decreases due to absorption by doped f-CNTs [30]. In the photographic images, the scattering level is not clearly expressed though it is clearly seen in UV-Visible transmittance profile. All OILC samples experience the incident light scattering [17], but the absorption is realized only for f-CNT doped samples causing reduced transmittance with a concentration of f-CNTs because $\beta$ increases with increasing f-CNT doped although $d$ is fixed.

The effect of doped f-CNTs on the polymer nanostructure was investigated using FE-SEM. In order to get avoid cracks and breakage on the polymer network, firstly, the test cells were soaked in n-hexane for one day and then the substrates were separated with a sharp-edged blade. Once again, the OILC film with substrate was soaked for one more day, and polarizing optical microscopy was used to confirm the absence of LC in the film. Thereafter, to avoid charge accumulation on the polymer film while taking the images, a conductive platinum film was overcoated onto the polymer surface by RF sputtering. Obtained micro-images with relative droplet size distributions are depicted in Fig. 5. The droplet size distribution is estimated using an image analyzer software, Image-J (a Java-based Image processing developed at the National Institute of Health), and obtained data with Gaussian fits are illustrated inset of Fig. 5. The Gaussian fits exhibit peaks around 211, 215, 210 and 208 nm depicting the average droplet sizes of the samples S1, S2, S3 to S4, respectively. Very few droplet sizes above visible wavelength regime i.e. 350 nm are also found, causing some level of light scatterings in the visible regime, especially in short wavelengths. Few droplets whose size is below 100 nm has also been observed in samples, which renders the device to have a high driving voltage to induce maximum birefringence since $V_{th} \propto 1/R$. Additionally, doping of f-CNT does not show any appreciable variation on the surface morphology of the polymer network though the average droplet size decreases slightly with increasing doping weight percent of f-CNTs.

### 4.2. Electro-optic properties

Initially, we have observed OILC cells under an optical microscope.

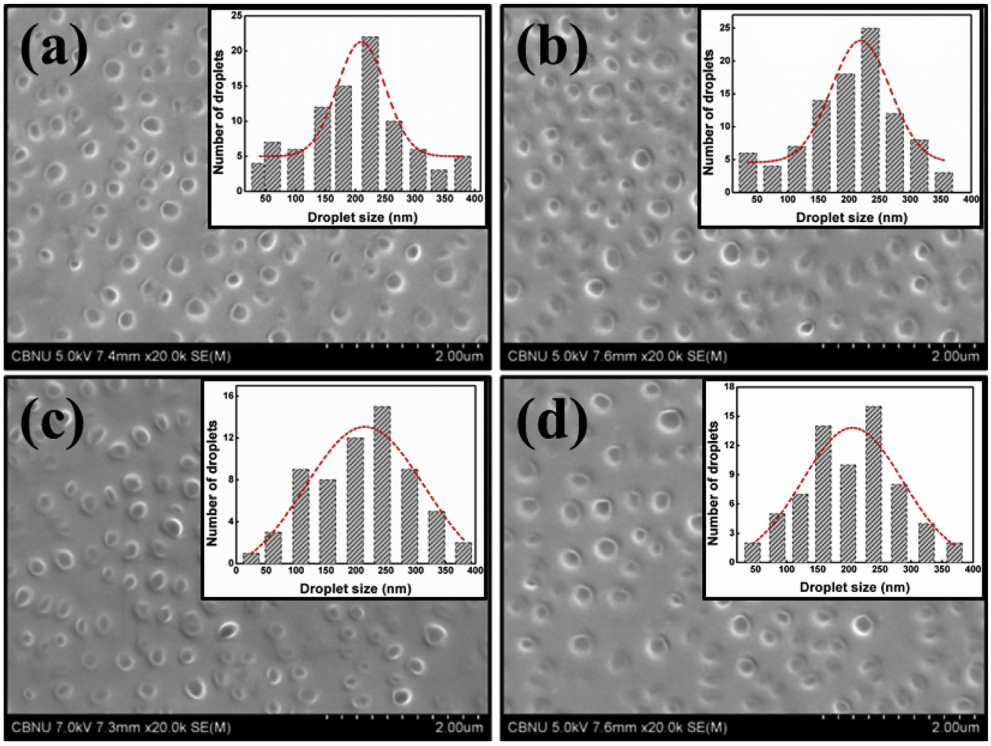


**Fig. 5.** FE-SEM of the polymer networks with various concentrations of f-CNTs (b) S2, (c) S3 and (d) S4 are compared with (a) conventional OILC, S1, and the resultant droplet size distributions with the Gaussian fit.

The cells filled with S2 and S3 do not exhibit dark spots associated with agglomeration of f-CNTs, indicating the size of CNT-aggregates is at least less than 1 μm. However, a few dark spots were observed in S4 cell in which a maximum amount of f-CNT, 0.01 wt. % is loaded into.

After the preliminary investigation, we have observed the light leakages and field-induced birefringence of the OILC samples by placing the cells between crossed polarizer in POM. Then the isotropic phase was confirmed by rotating the sample's plane between the crossed polarizers. All samples appeared black, exhibiting optically isotropic phase at field-off state. However, a feeble light scattering is realized in the sample S1 due to mismatching of the refractive indices between interfaces of the LC/polymer networks and few larger droplets inside the composite film. Though, the feeble light scattering was found to be minimized considerably with the effect of the doped f-CNTs.

In order to perform quantitative analysis of the reduced light leakages associated with the effect of doped f-CNTs for all samples, multiple optical images of each sample at different positions were captured with the invariable intensity of incident light. Then, the obtained results are compared using the mentioned image analyzer, in which the perfect dark level is predefined as “0” by the software. As all the measured light leakages are in arbitrary units, we have examined several positions in each sample and taken an average of many different unit areas for each sample. The statistical mean value along with standard deviations from the mean of the illumination for the samples from S1 to S4 are 30.9 ± 1.04, 18.1 ± 0.86, 11.6 ± 0.98 and 8.1 ± 1.3, respectively. This implies, when compared with the conventional OILC S1, the feeble light leakages for the sample S2 to S4 are decreased gradually by 1.7, 2.6 and 3.8 times respectively, indicating the dark level of the device is improved with the increasing concentration of the dopant. As the material concentrations and UV polymerization kinetics include temperature, irradiation intensity and irradiation time kept invariant for all samples, we anticipate that the variation of light leakages is attributed to the f-CNT dopant in the composite medium. We also compared the dark level with vertical alignment (VA) LC mode which gives a better dark state in comparison with other basic LC modes such as twisted nematic and homogeneous alignment modes. The VA cell with use of the same LC and with a cell gap of 4.5 μm exhibited a light leakage of 13.1 ± 0.11, indicating the sample S3 and S4 exhibit excellent dark state too compared to that of conventional VA mode.

According to Beer's law, the absorption and scattering occur simultaneously when the incident light passes through the composite; therefore, the intensity of transmitted light is decreased. The contrast ratio is defined as the ratio of the transmission intensity of bright state to the transmission intensity of the dark state. As the contrast ratio and light leakages are inversely proportional to each other, hence, the decreased light leakages in the field-off state lead to enhanced contrast ratio. A similar kind of increased contrast ratio with reduced light leakages is reported in the literature [13,17,23]. On the other hand, upon switching on the electric field, the randomly oriented LC directors inside LC droplets tend to align along the field direction, giving rise to induced birefringence. As a result, a uniform transmittance is observed between the electrode gaps, as shown in Fig. 6. This shows the maximum transmittance between electrodes is slightly increased from S2 to S4 when compared with the conventional OILCs of S1 while the same voltage is applied to all cells. The origin of increased transmittance at the same applied voltage is associated with a decrease in the $V_{th}$ in the f-CNTs doped cells, originating from the effective field strength experienced by LC within droplets significantly increases with the concentration of doped f-CNTs.

In order to investigate the switchable electro-optic properties associated with the f-CNTs doped OILCs, we have measured transmittance as a function of applied voltage as shown in Fig. 7. In sample S1, the transmittance observed under crossed polarizers in a voltage-off state is quite deviated from baseline due to feeble light scattering [17]. However, in samples from S2 to S4, a better dark level was achieved due to absorption of the incident polarized light propagating through embedded f-CNTs in doped samples. Besides, the dark level decrease with the concentration of doped f-CNTs such that the total amount of propagated incident light through the composite is decreased to 1.6, 2.1 and 3.7 times from samples S2 to S4, respectively, in comparison with

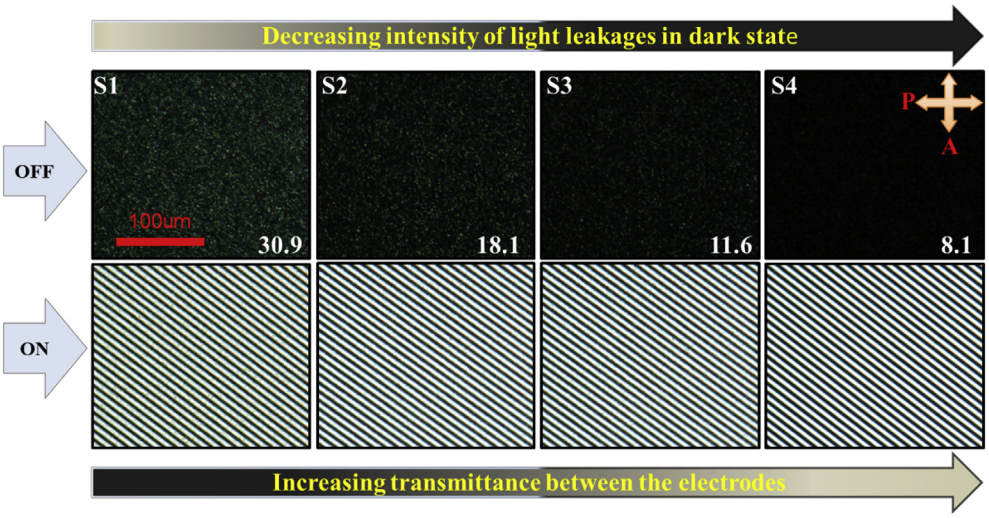


**Fig. 6.** POM images of the dark and bright states were taken between the crossed polarizers. The numbers inside images of dark state represent relative brightness. The applied field is $50V_{rms}$.

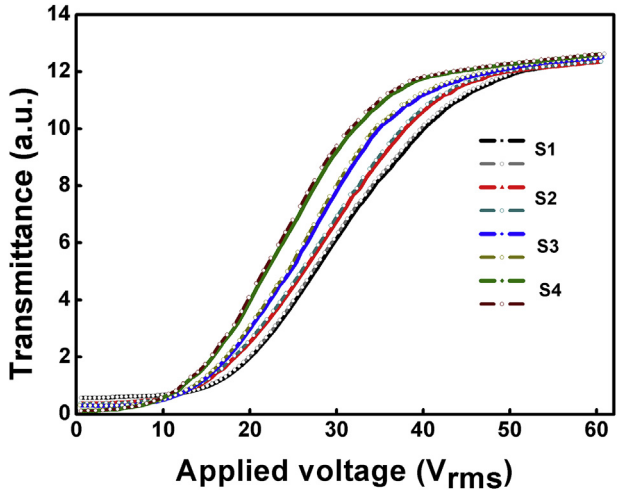


**Fig. 7.** Voltage-dependent transmittance curves of the OILC and its f-CNT doped composite samples. The solid straight and dotted lines indicate increasing and decreasing of the fields, respectively, and the transmittance are measured under the crossed polarizer with an incident light wavelength of 633 nm.

**Table 1**
The threshold voltage ($V_{th}$), operating voltage ($V_{op}$), hysteresis (H) and relative light leakages in the dark state as a function of the concentration of doped f-CNTs. LC=45%

| Sample name | $V_{th}$ (10%) ($V_{rms}$) | $V_{op}$ (90%) ($V_{rms}$) | H (%) | Relative light leakage[a] |
|---|---|---|---|---|
| S1 | 16.6 | 45.63 | 0.202 | 0.592 |
| S2 | 15.47 | 43.18 | 0.211 | 0.383 |
| S3 | 14.65 | 40.90 | 0.206 | 0.294 |
| S4 | 12.86 | 37.09 | 0.209 | 0.161 |

[a] Herein, the relative light leakage was measured with the wavelength of incident light 633 nm.

the conventional one as indicated in Table 1. On the other hand, when the voltage is applied, the transmittance increases for all samples and saturates at a higher voltage, indicating the induced birefringence reaches the half-wave plate. We have quantified the threshold voltage ($V_{th}$), operating voltage ($V_{op}$), hysteresis (H) and relative feeble light leakages at voltage-off state, as shown in Table 1, where the $V_{th}$ and $V_{op}$ are defined as the voltage required for reaching 10% and 90% transmittance of the total transmittance, respectively. A significant reduction in $V_{th}$ viz. 6.8, 11.74 and 22.5% and $V_{op}$ viz. 5.36, 10.36 and 18.71% is achieved for samples S2, S3, and S4, respectively, when compared to conventional OILC, S1.

In addition, we have also measured the electro-optic hysteresis (*H*) from the voltage-dependent transmission curves as depicted in Fig. 8. Herein, the *H* is defined as applied voltage difference between increasing and decreasing field swipes at 50% transmittance ($\Delta V_{T50\%}$) normalized by voltage at saturated transmission ($V_{T100\%}$) and thus it could be expressed as $H(\%) = \frac{\Delta V_{T50\%}}{V_{T100\%}} X100$, and the calculated *H* values are depicted in Table 1. All samples do not show any considerable indication of the *H*, unlike the polymer-stabilized blue phase (PSBP), and the f-CNTs-doped samples exhibit significantly negligible loops as compared to the conventional OILCs. This indicates that the nanostructured LC droplets reorient along the field direction, on field application, and then relaxes to the regular position in the field-off state. The possible reason for relaxation is the strong anchoring from the interface between the LC/polymer networks. Therefore, we expect that doping f-CNTs into the system does not interrupt the anchoring energy and morphology of the droplet size much because the hysteresis mainly relies on those factors.

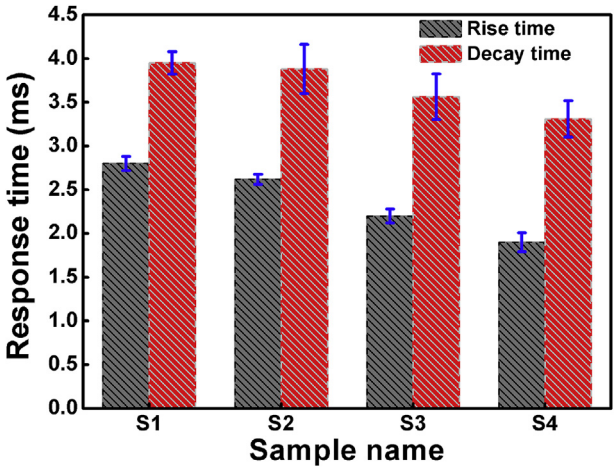


**Fig. 8.** The response times of the f-CNTs doped OILC is compared with conventional OILC, (S1) for measuring response time we have applied $60V_{rms}$ with a square wave of 1 KHz for all samples.

Furthermore, we have investigated the effects of f-CNT doping on response times. The rise and decay times are defined as the time elapsed for the transmittance to increase from 10% to 90% of maximum and the time elapsed for the transmittance to decrease from 90% to 10% of minimum, respectively. The average response times of f-CNT doped samples are exhibited as column diagram in Fig. 8 with estimated standard error bars. The obtained response times are measured with the same applied voltage for all samples. Faster response time is achieved with increasing doped weight percent of f-CNT from sample S1 to S4 such that for the samples S2, S3, and S4 the measured rise times are faster by 7, 21 and 35% and the decay times ($\tau_{off}$) are faster by 3, 12 and 19% compared with the conventional OILC, S1.

In general, the conventional OILC shows fast response times due to their finite coherence length because the LC is confined into nano-sized pores and strong anchoring between interfaces of the LC/polymer network. Interestingly, the f-CNT doped samples exhibit faster rise times as concentration of f-CNTs goes high when we applied the same fields for all samples because the embedded f-CNTs offer field enhancement effect, in the field-on state. The two-step ($V < V_{th}$ and $V > V_{op}$) reorientation phenomenon of the LC molecules in the nano-sized droplets with the effect of applied fields was reported in the literature which shows reorientation of LC molecules mainly relies on the applied fields [31]. Therefore, the field enhancement with the effect of f-CNTs would strongly emphasize that the f-CNTs allow more field strength to act on the polymer encapsulated LC droplets as compared to conventional one when the applied fields are the same for all samples. Conversely, in $\tau_{off}$, the director relaxation could be controlled by both the viscoelastic properties of the host LC $\gamma_1/k_{eff}$ and the LC confinement size $R$. In OILC, the $k_{eff}$ is the resultant of both bend $k_{33}$ and splay $k_{11}$ deformations. The measured $\tau_{off}$ from the samples S1 to S4 are 3.95, 3.88, 3.56 and 3.31 ms, respectively, as shown in Fig. 8. As mentioned in the switching mechanism, the reduction of $\tau_{off}$ can occur when $R$ becomes smaller or $\gamma_1/k_{eff}$ is reduced by increased $k_{eff}$. Considering the droplet size change only on $\tau_{off}$, 3.95 ms for S1 should be 3.91 ms and 3.84 ms for S3 and S4, respectively. However, the measured values 3.56 and 3.31 ms for S3 and S4 is much shorter than the estimated values which considers the droplet size reduction effect only. The difference between the measured and calculated $\tau_{off}$ could be anticipated that the short-range elastic interaction is realized between interfaces of LC and f-CNT inside the polymer encapsulated LC droplet. Therefore, we conclude that the enhanced elastic constants by doped f-CNTs contributes partly to faster $\tau_{off}$ in f-CNT doped samples [27].

In the proposed approach, the LC to monomer ratio and polymerization kinetics is unaltered, therefore we believe that the enhanced fast switchable electro-optic responses such that $V_{th}$, $V_{op}$ and rise time are purely from the enhanced field strength, whereas the $\tau_{off}$ might be from combined effect of reduced droplet size and increased elastic constant by the embedded f-CNTs. Similar kinds of performances in polymer dispersed liquid crystals are reported in the literature [32]. The proposed current scheme might have improved even further if the addition of the f-CNT is not limited by agglomeration tendency in the highly viscous pre-polymer.

## 5. Conclusions

We have proposed incorporation of a small amount of conductive f-CNTs into the conventional OILCs, in which the composite films were prepared by varying the concentration of f-CNTs using a well-known polymerization induced phase separation method. The conducting f-CNTs interconnects between LC encapsulated polymeric droplets giving rise to the field enhancement effect in the composite, thereby, the $V_{th}$ and $V_{op}$ were significantly reduced. In addition, the switching on and off times were also found to be faster. In the field-off state, f-CNT doped samples exhibit minimized feeble light scattering between the crossed polarizers in comparison with pure OILCs owing to absorption of the scattered light by f-CNTs. The improved performances of the fast switchable electro-optics would contribute to the upcoming technologies for the flexible liquid crystal display and photonic devices.

## Acknowledgment

This research was supported by the Basic Science Research Program through the National Research Foundation of Korea (NRF) funded by the Ministry of Education (2016R1A6A3A11930056 and 2016R1D1A1B01007189).

## Appendix A. Supplementary data

Supplementary data to this article can be found online at https://doi.org/10.1016/j.compositesb.2019.01.091.

## References

[1] Kim MS, Lim YJ, Yoon S, Kang SW, Lee SH, Kim M, Wu ST. A controllable viewing angle LCD with an optically isotropic liquid crystal. J Phys D Appl Phys 2010;43(14):145502.
[2] Choi SW, Yamamoto SI, Iwata T, Kikuchi H. Optically isotropic liquid crystal composite incorporating in-plane electric field geometry. J Phys D Appl Phys 2009;42(11):112002.
[3] Bahadur B. Liquid crystals: applications and uses. World Scientific; 1990.
[4] Park NH, Noh SC, Nayek P, Lee MH, Kim MS, Chien LC, Lee JH, Kim BK, Lee SH. Optically isotropic liquid crystal mixtures and their application to high performance liquid crystal devices. Liq Cryst 2015;42(4):530–6.
[5] Rao L, Ge Z, Wu ST, Lee SH. Low voltage blue-phase liquid crystal displays. Appl Phys Lett 2009;95(23):231101.
[6] Yang YC, Yan DK. Electro-optic Kerr effect in polymer-stabilized isotropic liquid crystals. Appl Phys Lett 2011;98(2):023502.
[7] Haseba Y, Kikuchi H, Nagamura T, Kajiyama T. Large electro-optic Kerr effect in nanostructured chiral liquid-crystal composites over a wide temperature range. Adv Mater 2005;17(19):2311–5.
[8] Aya S, Le KV, Araoka F, Ishikawa K, Takezoe H. Nano size-induced optically isotropic nematic phase. Jpn J Appl Phys 2011;50(5R):051703.
[9] West JL. Phase separation of liquid crystals in polymers. Mol Cryst Liq Cryst Incorp Nonlinear Opt 1988;157(1):427–41.
[10] Justice RS, Schaefer DW, Vaia RA, Tomlin DW, Bunning TJ. Interface morphology and phase separation in polymer-dispersed liquid crystal composites. Polymers 2005;46(12):4465–73.
[11] Matsumoto S, Houlbert M, Hayashi T, Kubodera KI. Fine droplets of liquid crystals in a transparent polymer and their response to an electric field. Appl Phys Lett 1996;69(8):1044–6.
[12] Shin SJ, Cho NH, Lim YJ, Nayek P, Lee SH, Hong SH, Lee HJ, Shin ST. Optically isotropic liquid crystal mixture showing high contrast ratio and fast response time. Proceedings of IMID digest-11 conference. Korea. Oct, 2011. p. 139–40.
[13] Manda R, Pagidi S, Kim MS, Park CH, Yoo HS, Sandeep K, Lim YJ, Lee SH. Effect of monomer concentration and functionality on electro-optical properties of polymer-stabilized optically isotropic liquid crystals. Liq Cryst 2017;45(5):736–45.
[14] Rao L, Yan J, Wu ST, Yamamoto SI, Haseba Y. A large Kerr constant polymer-stabilized blue phase liquid crystal. Appl Phys Lett 2011;98(8):081109.
[15] Zhu JL, Ni SB, Song Y, Zhong EW, Wang YJ, Ping Chen C, Ye Z, He G, Wu DQ, Song XL, Lu JG. Improved Kerr constant and response time of polymer-stabilized blue phase liquid crystal with a reactive diluent. Appl Phys Lett 2013;102(7):071104.
[16] Kizhakidathazhath R, Higuchi H, kumura Y, Kikuchi H. Weak anchoring interface inducing acrylate copolymer designs for high-performance polymer-stabilized blue phase liquid crystal displays. ChemistrySelect 2017;2(23):6728–31.
[17] Pagidi S, Manda R, Lim YJ, Song SM, Yoo H, Woo JH, Lin YH, Lee SH. Helical pitch-dependent electro-optics of optically high transparent nano-phase separated liquid crystals. Opt Express 2018;26(21):27368–80.
[18] Lim YJ, Yoon JH, Yoo H, Song SM, Manda R, Pagidi S, Lee MH, Myoung JM, Lee SH. Fast switchable field-induced optical birefringence in highly transparent polymer liquid crystal composite. Opt Mater Express 2018;8(12):3698.
[19] Saito R, Dresselhaus G, Dresselhaus MS. Physical properties of carbon nanotubes. 1998.
[20] Rao CNR, Satishkumar BC, Govindaraj A, Nath M. Nanotubes. ChemPhysChem 2001;2(2):78–105.
[21] Rahman M, Lee W. Scientific duo of carbon nanotubes and nematic liquid crystals. J Phys D Appl Phys 2009;42(6):063001.
[22] Lynch MD, Patrick DL. Organizing carbon nanotubes with liquid crystals. Nano Lett 2002;2(11):1197–201.
[23] Yu JH, Lee JJ, Lim YJ, Nayek P, Kundu S, Kang SW, Lee SH. Optically isotropic polymer dispersed liquid crystal composite for high contrast ratio and fast response time. Proceedings of SID symposium digest of technical papers. Canada. May, 2013. p. 1338–40.
[24] Shin EJ, Noh SC, Kim TH, Kim JH, Nayek P, Lee MH, Kim MS, Chien LC, Lee JH, Kim BK, Lee SH. Enhancement of electro-optic properties of optically isotropic liquid crystal device for flexible display. Proceedings of SID symposium digest of technical papers. California. Jun, 2015. p. 1483–6.

[25] Amundson K. Electro-optic properties of a polymer-dispersed liquid-crystal film: temperature dependence and phase behavior. Phys Rev E 1996;53(3):2412.
[26] Lim YJ, Choi YE, Lee JH, Lee G-D, Komitov L, Lee SH. Effects of three-dimensional polymer networks in vertical alignment liquid crystal display controlled by in-plane field. Opt Express 2014;22(9):10634–41.
[27] Jeon SY, Shin SH, Jeong SJ, Lee SH, Jeong SH, Lee YH, Choi HC, Kim KJ. Effects of carbon nanotubes on electro-optical characteristics of liquid crystal cell driven by in-plane field. Appl Phys Lett 2007;90(12):121901.
[28] Wu JJ, Wang C-M, Li W-Y, Chen SH. Electro-optical properties of aligned dye doped polymer dispersed liquid crystal *f*ilms. Jpn J Appl Phys 1998;37(12R):6434–9.
[29] Montgomery Jr. GP, West JL, Tamura-Lis W. Light scattering from polymer-dispersed liquid crystal film: droplet size effects. J Appl Phys 1991;69(3):1605–16012.
[30] Kang BG, Lim YJ, Jeong KU, Lee K, Lee YH, Lee SH. A tunable carbon nanotube polarizer. Nanotechnology 2010;21(40):405202.
[31] Chang CM, Lin YH, Reshetnyak V, Park CH, Manda R, Lee SH. Origins of Kerr phase and orientational phase in polymer-dispersed liquid crystals. Opt Express 2017;25(17):19807–21.
[32] Lu L, Lu SY, Chien LC. Fast-switching electro-optical films based on polymer encapsulated liquid crystal, carbon nanotube, and dye. Proceedings of SPIE. California. Feb, 2009. p. 723204.